J Mater Sci (2006) 41:7288–7295
DOI 10.1007/s10853-006-0938-2

Production of single and multi-walled carbon nanotubes using natural gas as a precursor compound

R. Bonadiman · M. D. Lima · M. J. de Andrade · C. P. Bergmann

Received: 16 August 2005 / Accepted: 29 December 2005 / Published online: 26 October 2006

Abstract In this work, the Catalytic Chemical Vapor Deposition (CCVD) technique was used to synthesize carbon nanotubes (CNT). Natural gas (NG) was employed as a carbon source for the growing of CNT, while magnesium oxide was used as a catalyst support for the nanotubes synthesis. Two systems were utilized. The Fe–Mo/MgO system was obtained by the impregnation technique through the dispersion of iron oxide, which is the catalyst, over magnesia (with molybdenum additions). This system was tested intending to optimize the parameters for the production of single-walled carbon nanotubes (SWCNT). Moreover, $Mg_{1-x}Fe_xMoO_4$, which was prepared by the combustion synthesis method, was tested to produce multi-walled carbon nanotubes (MWCNT). The Fe-Mo/MgO tests were carried out under H_2/GN and Ar/GN atmospheres at 950 °C, whereas the $Mg_{1-x}Fe_xMoO_4$ was submitted to 1,000 °C under H_2/GN atmosphere. The Fe–Mo/MgO catalyst produced better results regarding number of CNT and their diameters under Ar/NG atmospheres than under H_2/NG atmospheres. The system $Mg_{1-x}Fe_xMoO_4$ produced MWCNT according to the expectations.

R. Bonadiman (✉) · M. D. Lima · M. J. de Andrade · C. P. Bergmann
Department of Materials Engineering, Federal University of Rio Grande do Sul, 99 Osvaldo Aranha Av. 705, 90035190 Porto Alegre, RS, Brazil
e-mail: renato@bonadiman.com.br

Introduction

Carbon nanotubes (CNT) are a new class of materials discovered in 1991 by S. Iijima [1], and they have attracted great interest from the scientific community because of their outstanding mechanical, electrical and thermal properties [2–4]. Several different processes regarding their synthesis have been successfully developed [5–10], and among the most important ones are laser ablation technique, graphite electrodes discharge and catalytic chemical vapor deposition (CCVD), the latter having the biggest potential for the mass production of CNT.

Despite CNT have been discovered 13 years ago, and the intense research that have been done, a cost-effective and high selectivity method for the CNT production has not been developed yet. Several authors have had success in CNT synthesis using numerous catalysts kinds [11–18], different atmospheres and temperatures. Colomer et al. [5] produced single-walled carbon nanotubes (SWCNT) with up to 170% of efficiency (considering the metallic catalyst mass) employing CH_4/H_2 atmospheres and Fe_2O_3 over MgO as a catalyst. Nevertheless, Lui et al. [6] also obtained good results (250% efficiency) in the synthesis of multi-walled carbon nanotubes (MWCNT) using Ar/H_2 atmospheres with the same catalyst developed by Colomer et al. [5]. There is a large variety of parameters in CNT synthesis process, but the most practical and/or efficient combination is yet unknown. The influence of parameters such as temperature, dilution gases and kind of hydrocarbon in systems like nanotubes synthesis over ceramic supports has not been systematically studied so far.

Recently, it was discovered by Kitiyanan et al. [7] that MoO_x (when added to catalysts containing Fe and/or Co) has the ability to reduce the diameter of the CNT produced by CCVD, favoring the formation of SWCNT.

Due to the low price and high availability of the natural gas (NG), its use can be of interest concerning the development of a high-scale, low-cost production of CNT. However, natural gas contains several different organic compounds and impurities (N_2, CO_2, H_2O); thus, the optimum adjustment of process parameters may demand considerable efforts.

In this paper, we report the evaluation of Fe–Mo/MgO catalyst in several atmospheres in order to optimize the parameters for SWCNT synthesis using NG as carbon precursor. Moreover, $Mg_{1-x}Fe_xMoO_4$ catalyst was tested aiming to produce MWCNT using NG as well.

Experimental procedure

The Fe–Mo/MgO catalysts were prepared by the impregnation method, according to Li et al. [8]. 12.3 g of commercial magnesia (Delaware) were mixed to an aqueous solution containing 8.08 g of $Fe(NO_3) \cdot 9H_2O$ and 0.205 g $(NH_4)_6Mo_7O_{24} \cdot 4H_2O$ dissolved in 200 ml of deionized water. The mixture was then stirred by ultra-sound during 40 min, and dehydrated at 110 °C during 24 h. The remaining powder was calcinated at 300 °C during 12 h.

The $Mg_{1-x}Fe_xMoO_4$ catalyst was made ready beforehand for the combustion synthesis method. $Mg(NO_3)_2 \cdot 6H_2O$, $(NH_3)_6Mo_7O_{24} \cdot 4H_2O$, $Fe(NO_3)_3 \cdot 9H_2O$ and citric acid were dissolved in distilled water to form a sol system. The amount of water was just enough to form such system. The proportions of $Fe(NO_3)_3 \cdot 9H_2O$, $Mg(NO_3)_2 \cdot 6H_2O$, $(NH_3)_6Mo_7O_{24} \cdot 4H_2O$ were calculated to satisfy the following molar ratio: Fe/Mg/Mo = 1:10:12. The resulting solution was then dried at 120 °C and calcinated for 30 min in air at 700 °C. The detailed preparation of the catalyst is described in Ref. [9].

The CNT synthesis was carried out in a mullite tubular reactor (Fig. 1), with 50 mm inner diameter and 500 mm long. The oven was externally heated by electrical resistances. The Fe–Mo/MgO catalysts were tested in the conditions 1–6, as shown in Table 1. Condition 7, also described in Table1, was used to test the $Mg_{1-x}Fe_xMoO_4$ catalyst 1. The carbon source was natural gas, and its composition is shown in Table 2. The synthesis of the CNT was carried out under room pressure. The catalysts were placed over an alumina substrate and located below the thermocouple inside the oven, as can be seen in Fig. 1. The system was heated from room temperature up to the synthesis temperature in 30 min; when the synthesis temperature was reached, the NGwas released inside the tube. After the synthesis time, the flux of NG was blocked, and the flux of carrying gas was raised to 400 l/h during 2 min, so the NG could be rapidly eliminated from the oven interior.

The characterization of the catalysts was firstly made by X-rays diffraction, using a Philips diffractometer model X'Pert MPD. It was equipped with a graphite monochromator and a copper anode, operating at 40 kV and 40 mA. A JEOL—JSM 580 scanning electron microscope and a JEOL—JEM 2010 transmission electron microscope were also employed for the materials characterization. Transmission electron microscopy (TEM) operated at 200 KV with a point resolution of 0.25 nm. In order to determine the oxidation temperatures of the carbonaceous materials, both differential thermal analysis (DTA) and thermogravimetric analysis (TGA) were carried out, using a Harrop equipment model ST-736. For these tests, 50 mg samples of carbonaceous mass were put onto a platinum crucible, the heating rate was approximately 5 °C/min up to 800 °C, and the air flux was approximately 20 l/h. Raman spectroscopy characterization was made at the High Pressures Laboratory of the UFRGS Physics Institute. The equipment used a He–Ne laser with excitation radiation of 632.8 nm. The BET surface area of the commercial magnesia was measured on a Quantachrome adsorption analyzer (Nova 1000), using N_2 as adsorbate at 77 K.

After synthesis, the Fe–Mo/MgO and $Mg_{1-x}Fe_xMoO_4$ samples with the carbonaceous mass were analyzed by means of scanning electron microscopy (SEM) and DTA. One group of Fe-Mo/MgO samples and the $Mg_{1-x}Fe_xMoO_4$ specimen were purified and then analyzed via TEM and Raman spectroscopy. The purification process consisted of immersion in HCl (36%—30 ml) at room temperature during 30 min under stirring. Subsequently, the acid was neutralized with a solution of Na_2CO_3, and the CNT were separated from the aqueous solution by filtration.

Results and discussion

Fe–Mo/MgO Catalyst

The diffractogram of the Fe–Mo/MgO catalyst after calcination can be seen in Fig. 2. The predominant phase is periclase (MgO), and the fact that iron and molybdenum formed a compound ($FeMoO_3$) indicates

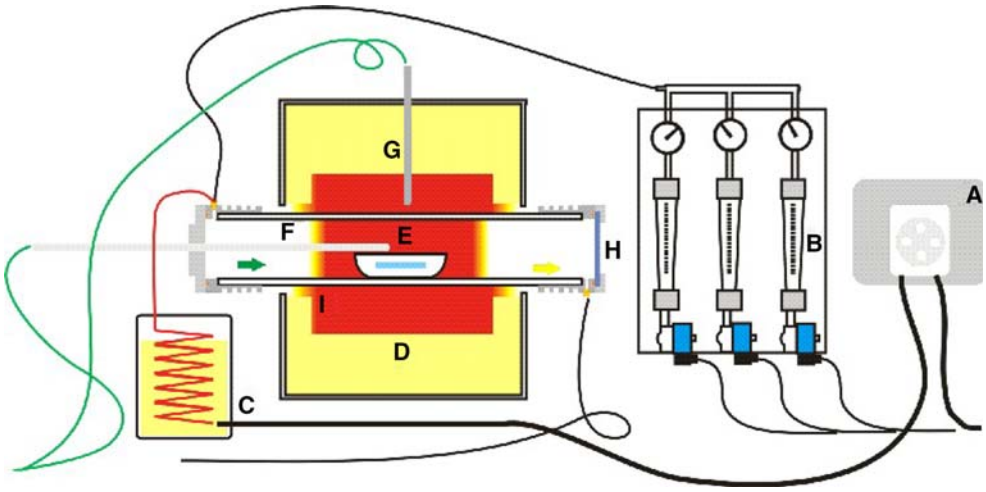

Fig. 1 Apparatus used for the CNT synthesis: (**A**) peristaltic pump for liquid precursors injection; (**B**) flow meters; (**C**) liquid precursors evaporator; (**D**) electric furnace; (**E**) substrate for growth of carbon nanotubes; (**F**) thermocouple; (**G**) mullite tube; (**H**) boron silicate view window

Table 1 CNT synthesis process parameters

Condition	Synthesis temperature (°C)	Synthesis t ime (min)	Ar (l/h)	NG (l/h)	H_2 (l/h)	Heating/ cooling gas
1	950	30	100	25	X	Ar
2	950	30	100	19	X	Ar
3	950	30	100	12	X	Ar
4	950	30	100	6	X	Ar
5	950	30	100	3	X	Ar
6	950	30	X	25	100	H_2
7	1,000	30	X	90	5	Ar

Table 2 Natural gas (NG) composition—volume %

Component		Volume %
Methane	CH_4	91.100
Ethane	C_2H_6	5.580
Propane	C_3H_8	0.970
Iso-Butane	C_4H_{10}	0.030
N-Butane	C_4H_{10}	0.020
Pentane	C_5H_{12}	0.100
Carbon dioxide	CO_2	0.800
Nitrogen	N_2	1.420

that a homogeneous mixture between these two metals has occurred. It can be noted that the oxidation states of iron were II and III, while for molybdenum it was III. The surface area, measured by means of BET analysis, was 105 m^2/g, and the mean pore size was 31 nm

The Fe–Mo/MgO catalyst produced better results regarding number of CNT and their diameters under Ar/NG atmospheres than under H_2/NG atmospheres, as seen in Fig. 3.

When comparing condition 6 (H_2/NG) to 1(Ar/NG), it can be noted that a lowest density of CNT was produced in condition 6. The produced CNT seem to be thicker when H_2 is used as a dilution gas. Probably, hydrogen led to an intense and quick reduction of Fe_2O_3 to metallic iron during heating and synthesis. The high amount of iron can cause agglomeration of these particles, which are larger than the optimum size for catalyzing CNT synthesis. Even tough some authors have reported the synthesis of CNT using Fe–Mo/MgO catalysts under CH_4 atmospheres [5, 12, 14, 19–24], the difference can be related to the characteristics of the catalyst support employed in this work. Colomer et al. [5] used a magnesium oxide with surface area of about 600 m^2/g and mean pore size around 3 nm. According to the principle concerning the synthesis of CNT over zeolites (Yang et al. [25]), pore diameters lower than 2 nm limit the growth of metallic particles and restrain the diameter of the formed CNT, but magnesia with pores below 5 nm can cause the same effect. Hydrogen also acts reducing carbon activity, favoring the hydrocarbon pyrolysis reaction to occur in the direction of carbon gasification, keeping carbon in gaseous phase. However, according to Li et al. [26] the excess of H_2 may hinder the NG decomposition reaction at higher temperatures. It may disturb the formation of SWCNT leading to a higher deposition of amorphous carbon.

Thermal analyses showed that there is a distinct oxidation behavior between samples of carbonaceous mass under Ar/NG and H_2/NG atmospheres, as can be observed in Fig. 4.

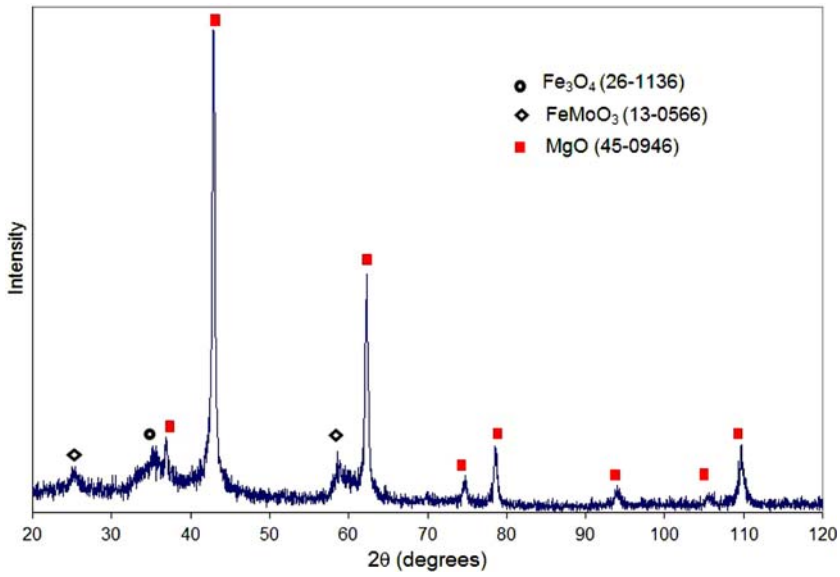

Fig. 2 X-ray diffraction of the Fe/Mo/MgO catalyst after calcination

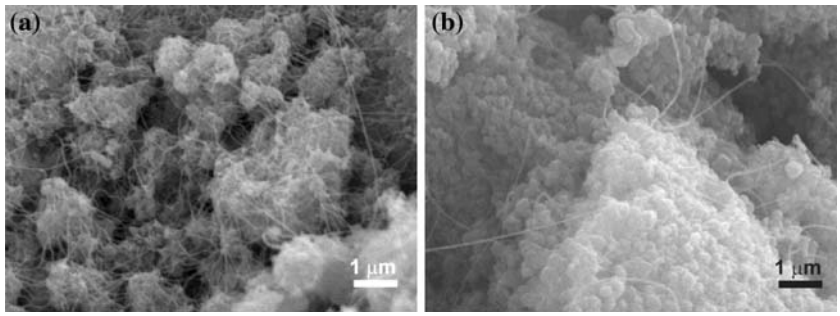

Fig. 3 Fe–Mo/MgO catalyst after CNT synthesis, under Ar/NG atmosphere—condition 1(**a**), and H_2/NG—condition 6 (**b**)

CNT samples synthesized under Ar/NG atmosphere (condition 1) had only one exothermic peak at 578 °C followed by an accentuated mass loss, while CNT samples synthesized under H_2/NG atmospheres (condition 6) had two peaks, at 458 °C and 571 °C, both occurring with mass loss. CNT had a different oxidation temperature than those of pyrolytic or amorphous carbonaceous mass. CNT generally oxidize in air under elevated temperatures. According to Gajewski et al. [27], the oxidation of amorphous carbonaceous mass occurs in a temperature range between 200 °C and 450 °C, and the CNT oxidize between 500 °C and 650 °C; however, these temperature ranges may vary with the process parameters, such as atmosphere, heating rate and the presence of metallic particles within the catalyst. Hence, the observed peaks between 500 °C and 650 °C (Fig. 4a, b) were probably caused by the oxidation of the CNT, while the peak at 460 °C (Fig. 4b) is attributed to the oxidation of amorphous carbon. Therefore, the use of H_2 as a dilution gas led to higher formation of amorphous carbon than with Ar.

The effect of the NG concentration on the CNT synthesis can be seen in Fig. 5. The reduction in the

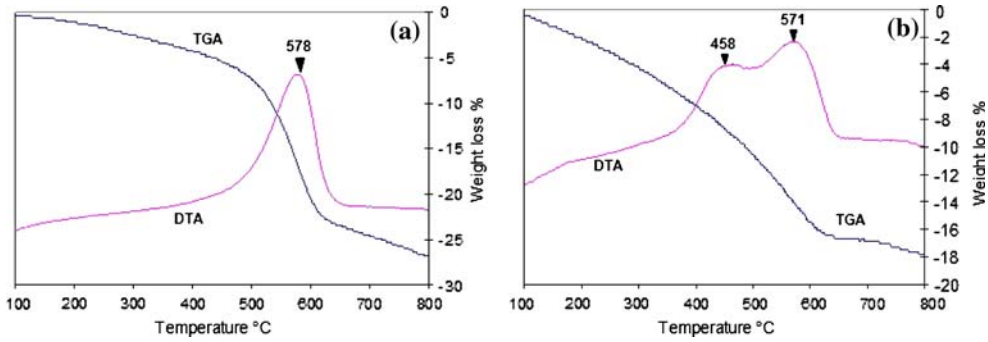

Fig. 4 Thermal analyses of carbon nanotubes synthesized under condition 1(**a**) and condition 6(**b**) over the Fe–Mo/MgO catalyst

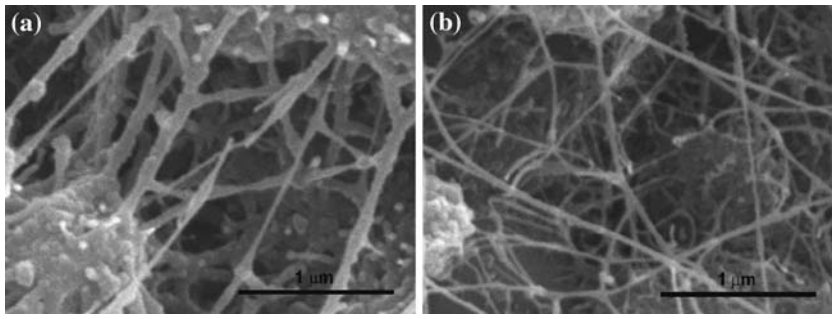

Fig. 5 SEM micrographs of CNT synthesized under conditions 2(**a**) and 4(**b**) over the Fe–Mo/MgO catalyst

hydrocarbons concentration resulted in the formation of thinner and ''cleaner'' CNT, i.e., with less amorphous carbon deposited over the nanotubes. Authors like Tang et al. [28], for instance, used high concentrations—between 20% and 25%—of diluted methane in Ar, and obtained CNT with low pyrolytic carbon deposition. However, since the NGused in this work contains heavier hydrocarbons (Table 2) that decompose in lower temperatures than methane, it was necessary to use low NG concentrations, in order to avoid excess of deposited amorphous carbon over the catalyst and the formed CNT.

The Raman spectra of CNT synthesized in conditions 4 and 2 are illustrated in Figs. 6 and 7, respectively. The centered peak at approximately 1,320 cm^{-1} is related to the band D, caused by the presence of defects in the structure of the sp^2 carbon. The degree of disorder of the nanotubes structure is generally low, and this band indicates deposition of amorphous carbon, or nanotubes with large diameters, or even nanofibers, which have more defects than nanotubes. The peak at around 1,580 cm^{-1} is related to the band G, which is generated by the tangential modes of vibration of carbon sp^2. Actually, it is intensified by the presence of nanotubes of small diameter, which have few defects. The ratio between the heights of the peaks G/D is 13 for condition 4 and 2.65 for condition 2. This is in agreement with the SEM analysis, indicating a better performance of the catalyst in lower NG concentration. Besides that, the asymmetry centered at 1,540 cm^{-1}, left to the band G, is associated with the presence of single-walled nanotubes [29]. Raman spectra indicate, for that reason, the existence of single-walled nanotubes of small diameter, but also the presence of disordered carbon, like thick nanotubes and non-catalytic amorphous carbon. The lower frequencies, between 100 cm^{-1} and 250 cm^{-1}, are denominated radial breathing mode (RBM). Peaks in this band are detected only when SWCNT and DWCNT are present [30]. It is also possible to estimate the diameter of the tubes using the formula [31]:

$$v(\mathrm{cm}^{-1}) = 12.5 + 223.5/d(\mathrm{nm})$$

where v is the wavelength of the peaks and d the diameter of the tubes. Using this equation, the diameters of the CNT were estimated between 1.2 nm and 2 nm.

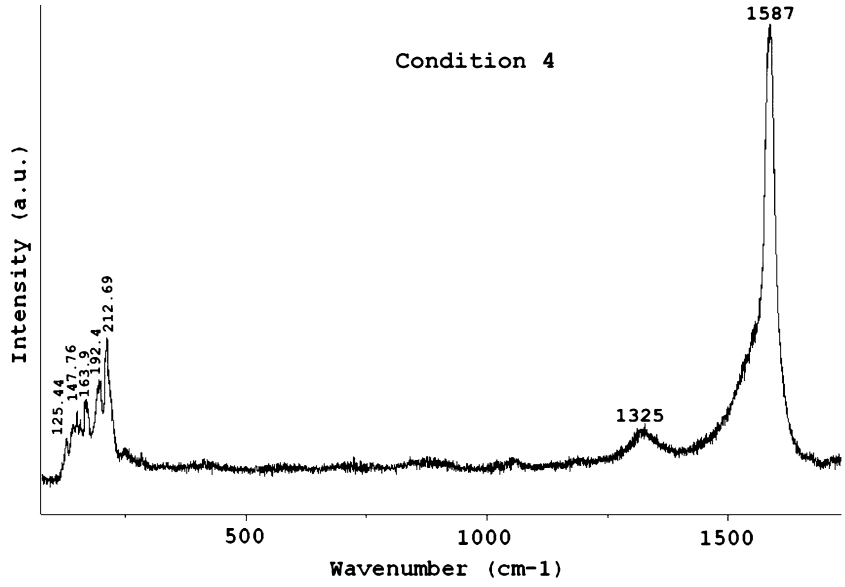

Fig. 6 Raman spectra of CNT synthesized using Fe–Mo/MgO catalyst under condition 4

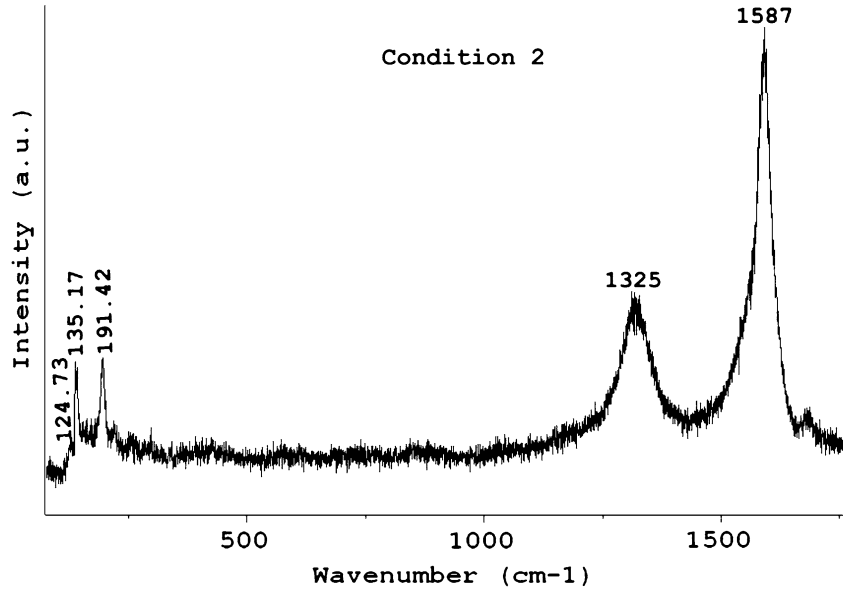

Fig. 7 Raman spectra of CNT synthesized using Fe–Mo/MgO catalyst under condition 2

Figure 8 shows the TEM micrograph of CNT synthesized in condition 1. It is possible to distinguish bundles of CNT formed by single and double walled carbon nanotubes with diameters between 0.6 nm and 1.8 nm. TEM characterization confirmed the results obtained by Raman spectroscopy.

$Mg_{1-x}Fe_xMoO_4$ Catalyst

The diffractogram of $Mg_{1-x}Fe_xMoO_4$ (Fig. 9) shows that the $MgMoO_4$ is the only specie visible. At normal conditions, Fe_2O_3–MoO_3 system can form $Fe_2(MoO_4)_3$ species after calcination [10]. However, the XRD pattern shows no Fe-containing phases, which probably implies that Fe ion entered into the $MgMoO_4$ lattice, and a solid solution must have been formed. The exchange of Fe^{3+} and Mg^{2+} in octahedral sites is one of the most important substitution in mineralogy. Cell parameters for normal $MgMoO_4$ are $a = 10.27$ Å, $b = 9.288$ Å, $c = 7.025$ Å, $\beta = 106.9°$, $v = 641.14$ Å^3, but measured cell parameters by XRD for our catalyst containing Fe are $a = 10.301$ Å, $b = 9.306$ Å, $c = 7.026$ Å, $\beta = 106.9°$, $v = 642.98$ Å^3. This slight enlargement in cell volume is associated to the possible replacement of Fe^{3+} cation on the site of Mg^{2+}. Thus, it is believed that the final catalyst could be written as Mg_{1-x} Fe_xMoO_4.

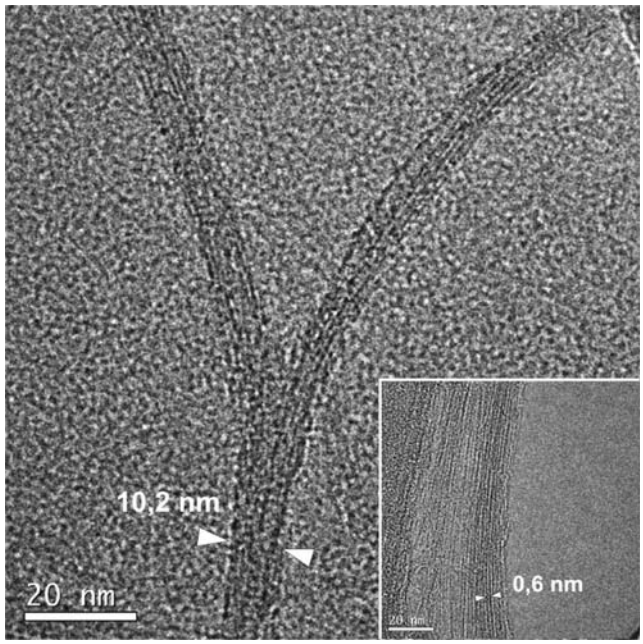

Fig. 8 TEM micrographs of CNT synthesized in condition 1. In the figure, it is possible to observe a bundle of nanotubes. Insert shows individual nanotubes forming the bundle

Figure 10 shows the thermal analyses of the products. This outcome should be originated by a great dispersion in the diameters of the MWCNT and by the presence of amorphous carbon. An accentuated mass loss between 500 °C and 700 °C corresponds to the oxidation of CNT and the amorphous material.

Figure 11 is a typical SEM image of the raw product synthesized over the $Mg_{1-x}Fe_xMoO_4$ catalyst by CVD method. There are hundreds of bundles that looked like lots of very fine fibers, and the diameters of the fibers are usually below 1 μm.

Raman spectroscopy is employed to investigate the quality and yield of the product. In Fig. 12, the relatively high ratio of IG/ID (1.94) indicates that the CNT are well graphitized. Peaks in the RBM band were not observed, indicating absence of SWCNT and DWCNT.

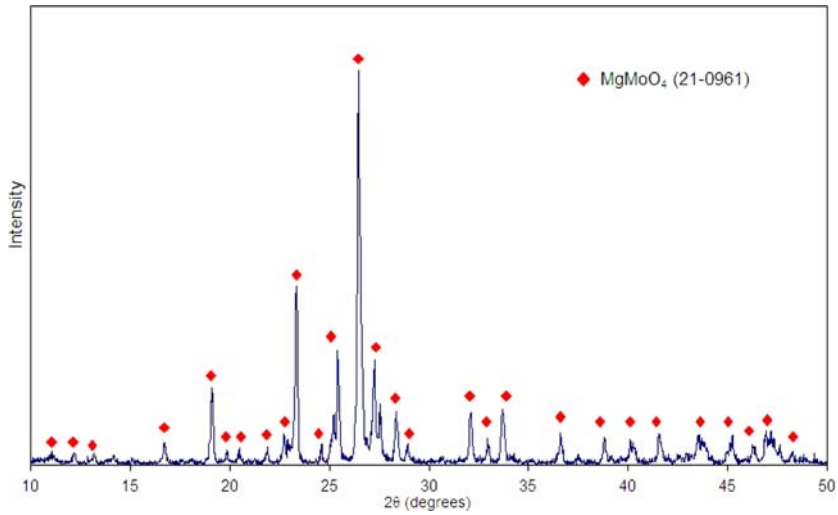

Fig. 9 X-ray diffraction pattern of the $Mg_{1-x}Fe_xMoO_4$ catalyst after calcination

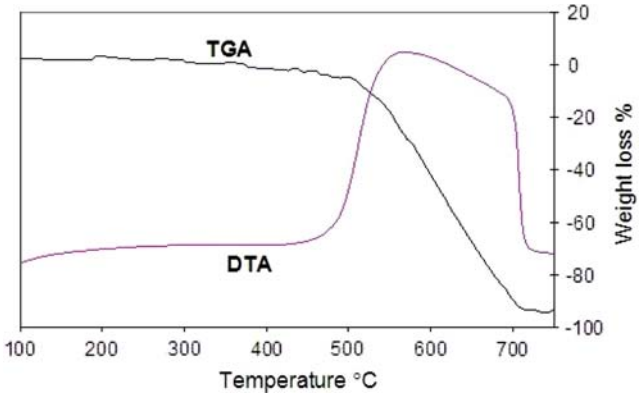

Fig. 10 Thermal analyses of carbon nanotubes synthesized under condition 7, over the $Mg_{1-x}Fe_xMoO_4$ catalyst

Figure 13 exhibits MWCNT with no metallic catalyst in their interior, which was probably removed away during treatment with acid. The diameter of

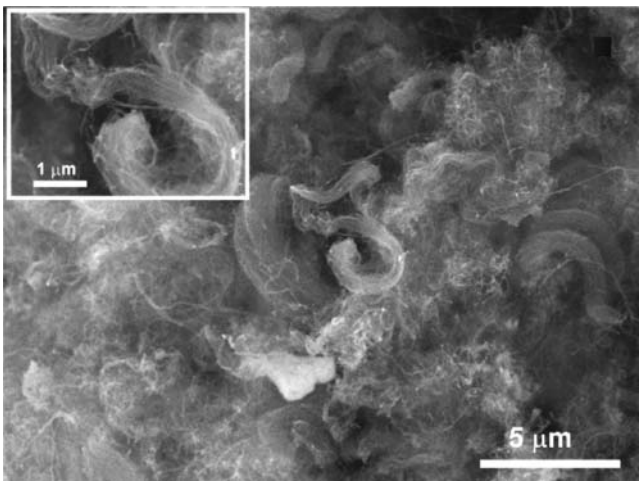

Fig. 11 SEM micrographs of CNT synthesized under condition 7 over $Mg_{1-x}Fe_xMoO_4$ catalyst

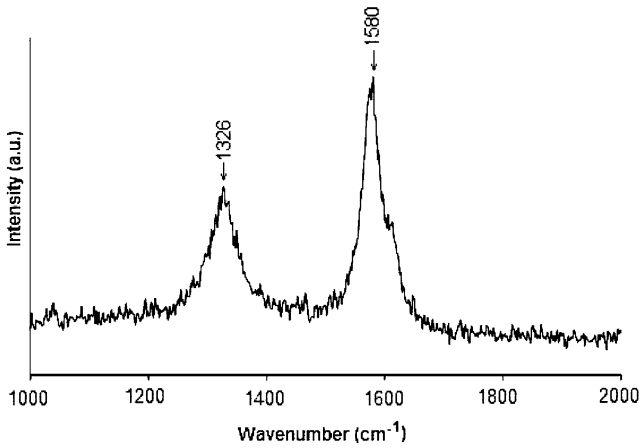

Fig. 12 Raman spectra of CNT synthesized under condition 7 over $Mg_{1-x}Fe_xMoO_4$ catalyst

MWCNT was between 40 nm and 80 nm. This transmission electron micrograph, similarly to the SWCNT, confirmed the result obtained by Raman spectroscopy.

Although some authors [32, 33] noticed that the presence of N_2 during the synthesis can cause the formation of nanotubes in cone form (carbon fibers with the graphitic plans forming one small angle with the axle), this was not observed in the transmission electron micrograph (Fig. 13).

Conclusions

Single and multi-walled carbon nanotubes could be synthesized using iron and molybdenum as catalysts and magnesium oxide as a ceramic support. The synthesis of nanotubes employing NGas a carbon source was really possible.

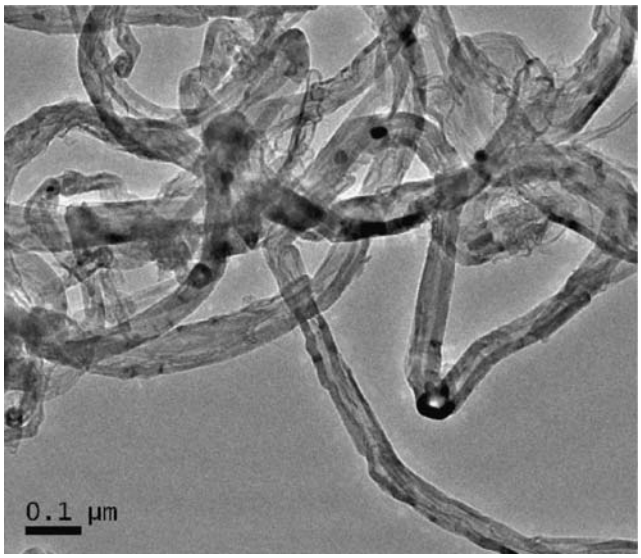

Fig. 13 TEM micrograph of CNT synthesized in condition 7

The efficiency of the SWCNT synthesis was higher under Ar/NG atmospheres than H_2/NG atmospheres when using magnesium oxide as a support. SWCNT with smaller diameters and less deposits of amorphous carbon were obtained when using less rich NG atmospheres, about 2.5%–5% volume. This concentration is lower than that used by other authors (20%–25% volume) to the synthesis on SWCNT in this temperature range. MWCNT was obtained using $Mg_{1-x}Fe_xMoO_4$ as catalyst and no optimization of the process parameters was necessary.

Acknowledgements Authors are grateful to the members of Laboratory of Ceramic Materials (LACER) for their contribution to the development of this study, to the CME/UFRGS (Electron Microscopy Center of the Federal University of Rio Grande do Sul) staff, who made the SEM and TEM analysis possible, and to the High Pressures Laboratory of the UFRGS Physics Institute personnel.

References

1. Iijima S (1991) Nature 354:56
2. Dresselhaus MS, Dresselhaus G, Eklund PC (1996) In: Science of fullerenes and carbon nanotubes. Academic press, San Diego, p.756
3. Ajayan PM (1999) Chem Rev 99:1787
4. Cumings J, Zettl A (2000) Science 289:602
5. Colomer JF, Stephan C, Lefrant S, Van Tendeloo G, Willems I, Konya Z, Fonseca A, Laurent Ch, Nagy JB (2000) Chem Phys Lett 317:83
6. Liu BC, Lyu SC, Lee TJ, Choi SK, Eum SJ, Yang CW, Park CY, Lee CJ (2003) Chem Phys Lett 373:475
7. Kitiyanan B, Alvarez WE, Harwell JH, Resasco DE (2000) Chem Phys Lett 317:497
8. Li S, Jiang F, Fan G, Wang L, Xiong C, Peng X, Mo H (2004) J Lumin 106:219
9. Li Y, Zhang XB, Tao XY (2003) A way of preparation of metal catalyst and its use in growth of bundled MWCN, Chinese Patent 03116514.1
10. Kuang WX, Fan YI, Chen Y (2000) Langmuir 16:1440
11. Dai H, Rinzler AG, Nikolaev P, Thess A, Colbert DT, Smalley RE (1996) Chem Phys Lett 260:471
12. Kong J, Cassell AM, Dai H (1998) Chem Phys Lett 292:567
13. Hafner JH, Bronikowski MJ, Azamian BR, Nikolaev P, Rinzler AG, Colbert DT, Smith A, Smalley RE (1998) Chem Phys Lett 296:195
14. Flahaut E, Govindaraj A, Peigney A, Laurent Ch, Rousset A, Rao CNR (1999) Chem Phys Lett 300:236
15. Cassell AM, Raymakers JA, Kong J, Dai H (1999) J Phys Chem B 103:6484
16. Colomer JF, Bister G, Willems I, Kónya Z, Fonseca A, Van Tendeloo G, Nagy JB (1999) Chem Commun 14:1343
17. Flahaut E, Peigney A, Laurent Ch, Rousset A (2000) J Mater Chem 10:249
18. Colomer JF, Stephan C, Lefrant S, Van Tendeloo G, Willems I, Kónya Z, Fonseca A, Laurent Ch, Nagy JB (2000) Chem Phys Lett 317:83
19. Ren W, Li F, Chen J, Bai S, Cheng HM (2002) Chem Phys Lett 359:196
20. Harutyunyan AR, Pradhan BK, Kim UJ, Chen G, Eklund PC (2002) Nano Lett 2:525
21. Geng J, Singh C, Shephard DS, Shaffer MSP, Johnson BFG, Windle AH (2002) Chem Commun 22:2666
22. Su M, Zheng B, Liu J (2000) Chem Phys Lett 322:321
23. Li WZ, Wen JG, Sennett M, Ren ZF (2003) Chem Phys Lett 368:299
24. Liu BC, Tang SH, Yu ZL, Zhang BL, Chen T, Zhang SY (2002) Chem Phys Lett 357:297
25. Yang Y, Hu Z, Lü YN, Chen Y (2003) Mater Chem Phys 82:440
26. Li Q, Yan H, Zhang J, Liu Z (2004) Carbon 42:829
27. Gajewski S, Maneck H-E, Knoll U, Neubert D, Dorfel I, Mach R, Strauß B, Friedrich JF (2003) Diamo Rel Mater 12:816
28. Tang S, Zhong Z, Xiong Z, Sun L, Liu J, Lin J, Shen ZX, Tan KL (2001) Chem Phys Lett 350:19
29. Kasuya A, Sasaki Y, Saito Y, Tohji K, Nishina Y (1997) Phys Rev Lett 78:4434
30. Maschmann MT, Amama PB, Goyal A, Iqbal Z, Gat R, Fisher TS (2006) Carbon 44:10
31. Li Y, Zhang X, Shen L, Luo J, Tao X, Liu F, Xu G, Wang Y, Geise HJ, Tendeloo VV (2004) Chem Phys Lett 398:276
32. Glerup M, Castignolles M, Holzinger M, Hug G, Loiseau A, Bernier P (2003) Chem Commun 20:2542
33. Suenaga K, Yudasaka M, Colliex C, Iijima S (2000) Chem Phys Lett 316:365